Published in final edited form as:
J Mol Neurosci. 2014 July ; 53(3): 525–536. doi:10.1007/s12031-014-0352-1.

lynx1 supports neuronal health in mouse dorsal striatum during aging: an ultrastructural investigation

Atsuko Kobayashi[1,2], **Rell L. Parker**[1], **Ashley P. Wright**[3], **Hajer Brahem**[3], **Pauline Ku**[3], **Katherine M. Oliver**[4], **Andreas Walz**[3], **Henry A. Lester**[1], and **Julie M. Miwa**[1,4,*]

[1]California Institute of Technology, Biology Division, MC 156-29, 1200 E. California Blvd., Pasadena, CA 91125 USA

[2]Tokyo Institute of Technology, Earth-Life Science Institute, 2-12-1 IE-31 Ookayama, Meguro-ku, Tokyo 152-8551 Japan

[3]Ophidion, Inc. 2265 E. Foothill Blvd. Pasadena, CA 91107 USA

[4]Lehigh University, Department of Biological Sciences, Iacocca Hall B217, 111 Research Dr., Bethlehem, PA 18015 USA

Abstract

Nicotinic acetylcholine receptors have been shown to participate in neuroprotection in the aging brain. Lynx protein modulators dampen the activity of the cholinergic system through direct interaction with nicotinic receptors. Although lynx1 null mutant mice exhibit augmented learning and plasticity, they also exhibit macroscopic vacuolation in the dorsal striatum as they age, detectable at the optical microscope level. Despite the relevance of the lynx1 gene to brain function, little is known about the cellular ultrastructure of these age-related changes. In this study, we assessed degeneration in the dorsal striatum in 1-, 3-, 7-, and 13-month-old mice, using optical and transmission electron microscopy. We observed a loss of nerve fibers, a breakdown in nerve fiber bundles, and loss of neuronal nuclei in the 13-month-old lynx1 null striatum. At higher magnification, these nerve fibers displayed intracellular vacuoles and disordered myelin sheaths. Few or none of these morphological alterations were present in younger lynx1 null mutant mice, or in heterozygous lynx1 null mutant mice at any age. These data indicate that neuronal health can be maintained by titrating lynx1 dosage, and that the lynx1 gene may participate in a trade-off between neuroprotection and augmented learning.

Keywords

nicotinic acetylcholine receptors; cholinergic system; prototoxins; neurotoxins; neurodegeneration; plasticity; learning and memory

[*]Correspondence should be addressed: Julie M. Miwa, Lehigh University, Department of Biological Sciences, 111 Research Dr., Iacocca Hall, B-217, Bethlehem, PA, 18015, Phone: (610)758-3079, Fax: (610)758-4004, jmm312@lehigh.edu.

Introduction

Throughout life, the cholinergic system provides important control over a number of neurotransmitter systems that participate in a variety of brain functions (Miwa et al., 2011; Picciotto, 2003). Cholinergic activation can have beneficial effects, promoting plasticity, learning (Levin et al., 2005) (Picciotto et al., 1995), and neuroprotective mechanisms (Bordia et al., 2008; Quik et al., 2007; Ryan et al., 2001; Stevens et al., 2003). Overactivation of the cholinergic system, however, has been linked to cell death (Orb et al., 2004; Orr-Urtreger et al., 2000), whereas, conversely, hypoactivity of the cholinergic system has been linked with neurodegenerative conditions such as Alzheimer's disease (Albuquerque et al., 2009; Decker and McGaugh, 1991; Terry and Buccafusco, 2003). Epidemiological evidence supports an inverse correlation between smoking and neurodegenerative disorders such as Parkinson’s disease, implying a further connection between nicotinic acetylcholine receptors and neurodegeneration; smoking seems to provide some neuroprotection against Parkinson’s disease (Huang et al., 2007; Picciotto and Zoli, 2008). Titrating the amount of cholinergic activation is therefore critical for normal brain function and for neuronal health.

During normal aging, cholinergic neurons and specific nicotinic acetylcholine receptor subtypes are eliminated selectively or reduced (Albuquerque et al., 2009; Terry and Buccafusco, 2003). This loss is thought to underlie cognitive decline, which is not a pathology, but part of the aging process (Picciotto, 2003). In certain pathologies, such as Alzheimer's disease and other dementias, there is a selective loss of various nicotinic acetylcholine receptor subtypes (Albuquerque et al., 2009), cholinergic neurons (Decker and McGaugh, 1991; Schliebs and Arendt, 2011), or axons of cholinergic neurons (Geula et al., 2008), which all play a role in the clinical manifestation of these diseases. In neurodegenerative disorders, therapies using acetylcholinesterase inhibitors can augment the contribution of the cholinergic system in improving cognition (Terry and Buccafusco, 2003). These therapies inhibit the enzyme that breaks down the neurotransmitter acetylcholine, acetylcholinesterase, and thus raise overall acetylcholine levels in the brain. Balancing this activity is critical because moderate activation of the cholinergic system can enhance cognitive functions, whereas overactivation can be detrimental (Picciotto, 2003). Thus, this inverted U-shaped relationship between activity and function requires tight regulation (Miwa et al., 2011).

Nicotinic acetylcholine receptors are ligand-gated ion channels of the cholinergic system that have been implicated in neuronal degeneration (Terry and Buccafusco, 2003) and survival (Dajas-Bailador et al., 2000; Kaneko et al., 1997; Stevens et al., 2003). Activation of these receptors leads to a rise in intracellular Ca^{2+} levels (Berger et al., 1998), partially because some subtypes allow Ca^{2+} to flux directly into the cell (Yamauchi et al., 2011). Animal studies indicate a neuroprotective effect of nicotine on mouse models of neurodegeneration (Ryan et al., 2001), suggesting a role of nicotinic acetylcholine receptors in neuroprotective mechanisms (Picciotto and Zoli, 2008; Stevens et al., 2003). It is well known that regulation of the activity of the cholinergic system is important in protecting neurons as they age (Albuquerque et al., 2009; Terry and Buccafusco, 2003).

The toxin-like modulators of the lynx family provide promising avenues for manipulation of cholinergic system activation levels. Lynx molecules are endogenous proteins that bind tightly to nicotinic acetylcholine receptors and modulate their function (Ibanez-Tallon et al., 2002; Miwa et al., 1999; Tekinay et al., 2009). Lynx1KO mice exhibit elevated nicotinic receptor responses, greater plasticity (Morishita et al., 2010), and increased learning and memory (Miwa et al., 2006). Our previous study also showed that neurons from lynx1KO mice exhibit elevated intracellular Ca^{2+} levels and enhanced nicotine-evoked rises in Ca^{2+} (Miwa et al., 2006). Lynx1KO neurons, however, are also more susceptible to glutamate-mediated neurotoxicity, and nicotine neuroprotection in vitro is abolished. Optical microscopic examination revealed that homozygous lynx1KO mice at the age of 12 months and older display vacuoles in the striatum and brainstem. This vacuolation can be ameliorated by crossing lynx1KO mice to $\alpha 7$ or $\beta 2$ null mutant mice, indicating that nicotinic acetylcholine receptor subunits are downstream effectors of lynx1 signaling.

Despite the link between levels of nicotinic receptor activity and neuron vulnerability, the role of lynx1 in this vacuolating degenerative process is unknown. To date, no detailed examination of the pathological features in the lynx1 mouse model has been undertaken. We therefore investigated the degeneration in the dorsal striatum as a function of age using optical and transmission electron microscope (TEM) ultrastructural analyses. Using TEM, we found two types of degeneration occurring in the dorsal striatum. One is an external degeneration, which occurs at the level of fascicle disorganization, such as a loss of nerve fibers and a loss of neuronal cell bodies. The other is an internal degeneration, which appears to be a degenerative change in axoplasm of axon fibers. The fascicles were compact with distinct boundaries in wildtype brains, but were indistinct with fuzzy margins in lynx1KO brains. When we examined axon and nerve fibers in cross section within the fascicles using TEM, we discovered unusual morphological alterations such as disordered myelin sheaths, axoplasmic anomalies, and vacuoles.

We have reported that lynx mRNA levels can be regulated by environmental and other manipulations (Miwa et al., 2011). This opens up the possibility that the brain may be subjected to altered amounts of susceptibility to neuronal damage. To understand the role of lynx1 dosage in cholinergic activity, we compared the effect of partial removal of lynx1, exhibited in heterozygous mice, to complete removal of lynx1 as exists in homozygous knockout mice.

The lynx1KO animals were largely normal during development and into early adulthood. We found that lynx1KO animals over one year of age have clear ultrastructural differences in the striatum, but this is largely spared in the heterozygous mice. This age-related degenerative phenotype in lynx1KO mice implicates lynx1 in neuronal health during aging.

Materials and Methods

Animals

lynx1KO mice were maintained as a backcross on a C57BL/6 (Charles River) background for > 8 generations. Heterozygous lynx1KO mice were intercrossed to derive a mixture of wildtype, heterozygous and homozygous lynx1KO mice. Lynx1KO mice used in this study

were all homozygous for lynx1KO. Animals were treated according to the guidelines detailed in the *Guide for the Care and Use of Laboratory Animals*, at the OLAR facility, California Institute of Technology, IACUC protocol number 1386-10G. All samples (1, 3, 7 and 13 month old of wildtype and lynx1KO) were prepared and analyzed with the investigator blinded to genotype.

Electron Microscopic analyses

Adult mice were used to examine the ultrastructure of nerve fibers in the dorsal striatum. Animals were perfused transcardially with saline/heparin followed by 1.25% glutaraldehyde and 1.5% sucrose in 0.1 M phosphate buffer (PB). Brains were fixed and sectioned coronally at 60 μm thickness on a vibrating microtome with 5% sucrose in 0.1 M PB. Sections were then postfixed with 2.0% glutaraldehyde and 1.5% sucrose in 0.1 M cacodylate buffer (pH7.4). Osmolarity was maintained at ~400 mOs throughout the fixation process (Cragg, 1980). Sections were then incubated in 2% osmium tetroxide with 0.8% K ferricyanide and 5% sucrose in 0.1 M Na cacodylate buffer for one hour followed by 2% aqueous uranyl acetate prestaining for 30 minutes in darkness. Sections were dehydrated in an acetone series and then embedded in EMBed 812 (Electron Microscopy Sciences). The samples were then cut into 60 nm thin sections with a diamond knife (DiATOME) on a Leica Ultracut UCT ultramicrotome. The thin sections were collected on a TEM grid, then post-stained with a 2% uranyl acetate and Reynold's lead citrate. For TEM imaging we used a Tecnai T12 operating at 120 kV., equipped with a Gatan Ultrascan 2k X 2k CCD camera. For analysis in the dorsal striatum we acquired many images to create montages of fascicles. Micrographs were quantified using Illustrator and ImageJ software. The number of fascicles was determined using Cell Counter and area measurements (# of fibers/μm^2).

Quantitative PCR

Tissue was quickly dissected on a cooled dissecting surface and placed into RNAlater stabilization reagent (Qiagen). Tissue was homogenized using a Bullet Blender homogenizer (Next Advance) with RNAse free metal beads to disrupt tissue. Homogenized tissue was quickly centrifuged and RNA was purified from supernatant using RNeasy columns (Qiagen). RNA was analyzed on a Bioanalyzer and subjected to RT reactions using 500 ng RNA (Quanta BioSciences). qPCR was performed in triplicate using a lynx1 TaqMan assay with GAPDH and HPRT as reference genes (Life Technologies) at a cDNA concentration of 1 ng per well. Experimental design and analysis was performed as per MIQE guidelines.

Western Blot

Protein extracts were prepared using a buffer solution of 2% SDS and 2% BME in PBS. Tissue was homogenized using Bullet Blender homogenizer. Extracts were centrifuged and supernatants run out on a 7% SDS-PAGE gel. Gels were blotted onto nitrocellulose membranes and blocked with 5% milk in TBS-T. Primary antibodies were applied at 1:500 dilution, and secondary antibodies incubated at 1:1000. Quantitation was performed using Li-COR system to measure anti-lynx1 bands, normalized to the actin bands for each sample. Triplicate samples were analyzed for each mouse brain.

Immunohistochemistry

We conducted immuno-labeling using the avidin biotin complex (Spencer-Segal et al., 2011). 13 month old mice were perfused transcardially with saline/heparin followed by 4% paraformaldehyde / 0.1% glutaraldehyde in 0.1 M PB and post-fixed for 0.1 M PB and post-fixed for 2 h and then stored in 25 % sucrose/0.1 M PB overnight. Brains were sectioned coronally at 30 μm thickness on a vibrating microtome with 5% sucrose in 0.1 M PB. Sections were treated with 1% sodium borohydride in 0.1 M PB for 2×20 minutes followed by avidin/biotin blocking agent for 15 minutes each, and by blocking buffer (2% normal goat serum, 1% bovine serum albumin, 0.1% CWFS in phosphate buffer saline PBS), and then incubated in mouse anti-Neuronal NeuN (Chemicon) for three days at 4°C. The control sections were treated with nonspecific IgG (Sigma-Aldrich). Sections were washed with incubation buffer (0.1% BSA-*c* in PBS) for 30 minutes. The sections were then incubated in biotinylated goat anti-mouse IgG (H+L) antibody (Kirkegaard & Perry Laboratories, Inc.) for two days at 4°C in darkness. After washing with incubation buffer for 3×5 minutes, sections were post-fixed with 2% glutaraldehyde in 0.1 M PB for 15 minutes. Sections were then labeled with peroxidase-conjugated streptavidin (DAKO). Labeling was visualized with stable diaminobenzidine (Invitrogen) and hydrogen peroxide. Labeled sections mounted on slides were examined by a Leica DM2500P microscope with 10x and 63x objectives.

Images were imported into Photoshop and divided into quadrants. Quadrant files were imported into ImageJ and the number of NeuN positive cells were quantified using the Cell Counter plug-in. Numbers for each quadrant were averaged and analyzed using ANOVA with post-hoc Tukey honest significant difference (HSD) test.

Results

We performed a TEM evaluation of lynx1KO mouse striatum, an area of substantial disruption at the light microscopic level. Within the striatum, nerve fibers (marked as N in figures 1 and 2) run in compact bundles, which we refer to as fascicles (drawn in dotted lines). In coronal cross sections, the majority of these fascicles have distinct boundaries demarcating them from the striatal neuropil, which is the rest of the striatal tissue external to these fascicles. Our past histological studies of 6, 9, 12, 15 and 18 month old mice showed that lynx1KO animals start to exhibit vacuolar degeneration in the tissues of the dorsal striatum at 12 months of age. We therefore employed TEM to investigate the degeneration of striatal tissues in more detail in animals aged 1, 3, 7 and 13 months.

Loss of lynx1 in aging alters the shape of nerve fiber bundles, and their borders are no longer defined

We generated cross section montages of the nerve fiber bundles in the dorsal striatum. In 1 month old wildtype (figure 1A) and lynx1KO (figure 1B) mice, fiber bundles appeared largely similar. In 3 month old-mice, both the wildtype (figure 1C) and lynx1KO (figure 1D) mouse striata were unchanged from 1 month old striata; the packing density of bundles within lynx1KO mice resembled wildtype. In 7 month old-mice, fascicles appeared largely similar in the wildtype (figure 2A) and lynx1KO (figure 2B) and the density of nerve fibers (marked N in figures) within the fascicles continued to look largely similar between the two

genotypes, indicating that there were only subtle differences between wildtype and lynx1KO mice in dorsal striatum up to that point.

In 13 month old-mouse brains, however, there was a striking difference in the structures in the dorsal striatum (figure 2C, D). In the montages of lynx1KO mouse brains, there were no defined borders to the nerve fascicles (figure 2D). The borders of the fascicles were indistinct (marked "?" in figure 2D), discontinuous in places, and the nerve fibers within the fascicle were dispersed with gaps between them (figure 2D). In the wildtype mouse brains of the same age, the border of the fascicles continued to appear smooth and regular, and the overall geometries of these fascicles appeared contiguous and intact (figure 2C).

We quantified the nerve fiber density in striatal montages to compare young (1- and 3-month-old) vs. aged (13- month-old) brains (Fig. 2e). We found a significant effect by ANOVA [$F(3,11)=6.11$, $p<0.01$] when comparing the 13-month-old lynx1KO fiber density (M = 56.4%, SEM ± 9.3%) to that of 13 month old wild type (M =100.0%, SEM ± 5.8%), young wild type (M = 88.2%, SEM ± 11.0%), and young lynx1KO samples (M = 77.1%, SEM ± 4.2%). Data were normalized and presented as a percentage of the density in the 13-month-old wild-type condition. Post-hoc comparisons using the Tukey HSD test indicated that the mean score for the 13-month-old homozygous KO condition was significantly different from the 13-month-old wild-type condition ($p<0.01$). Because we did not detect significant differences in nerve fiber density between wild type and lynx1KO brains in young animals, we conclude that the reduction in nerve fiber density in the 13-month-old lynx1KO is a progressive effect that occurs during aging.

Aging lynx1KO mice exhibit internal disruptions within axon fiber bundles

At higher TEM magnification, we examined the nerve fibers within the fascicles. The nerve fibers were markedly different between the 13 month old lynx1KO (figure 3C and D) and age-matched wildtype sections (figure 3A and B). Whereas the wildtype axons had ordered myelin sheaths, the lynx1KO axons were highly disordered (marked SD in figure 3D). In addition, the extent of myelination appears to be reduced in the lynx1KO samples as compared to the wildtype samples. In the lynx1KO mice (figure 3C and D) some of the nerve fibers have vacuoles (marked NV in figure 3), which were not observed in the wildtype sections.

Aging lynx1KO mice display degeneration in striatal neurons

We wanted to ascertain whether the morphological alterations of aging lynx1KO brains were confined to nerve fibers traversing the striatum or if other sub-regions, such as the regions between the fascicles – the striatal neuropil - were also affected. We therefore performed TEM on the striatal neuropil, which contain relatively more cell bodies and fewer nerve fibers of passage than in the fascicular region. These regions contain dendritic (marked as DR in figure 4) and somatic (figure 5) structures. In the 13 month old sections of wildtype (figure 4A and B), it was evident that nerve fibers in the region were surrounded by a dense network of tissue containing many dendrites. The lynx1KO, however, exhibits a striking disruption in the striatal neuropil (figure 4C and D), with areas between dendrites and other structures having a very low density (marked E in figure 4C and D). Furthermore,

we saw signs of degeneration in the nucleus in the lynx1KO samples, with cases of both condensed nuclei and cleared nuclei (figure 5B). In the wildtype samples, however, the nuclei appeared to be intact with no condensation (figure 5A).

Age-related degenerative features are spared in heterozygous lynx1KO mice

Because of the severity of the phenotype in aged mice without lynx1, we wanted to determine if partial dosage of lynx1 would result in a less severe phenotype. We confirmed by qPCR analysis that heterozygous lynx1KO mice had a 50% reduction in lynx1 transcript levels in total brain extracts as compared to those of wildtype mice (figure 6C). We noted a corresponding reduction of lynx1 protein by Western blot analysis (figure 6A) from protein extracts of heterozygous brains compared to wildtype levels. Quantitative assessment indicates that lynx1 protein is expressed at about 50% of wildtype levels of protein (figure 6B).

We generated cross section montages of the fascicles in the dorsal striatum. Interestingly, in the 13 month old heterozygous mice (figure 7A) there was little evidence of such structural alteration as (?) can be observed in homozygous lynx1KO aging mice (figure 2D). At higher TEM magnification we examined the nerve fibers (marked as N in figure 7B) within the fascicles in the heterozygous lynx1KO mice. The heterozygous mice fibers had ordered myelin sheaths, same as the wildtype mice. In the striatal neuropil, the regions between the fascicles contain relatively few nerve fibers of passage (figure 7C). This tissue contained many dendrites (marked as DR in figure 7C) and was densely filled, as seen in the wildtype case. In the heterozygous lynx1KO mice, the nuclei appeared to be intact with no condensation (marked as Nucleus in figure 7A). Nerve fiber density measurements of fascicle montages did not show a significant difference between aged wildtype and heterozygous animals, while aged homozygous lynx1KO animals showed a significant reduction in nerve fiber density. There was a significant effect of genotype on fiber density at 13 months, at the $p<0.01$ level for the three conditions [$F(2,10)= 10.02$, $p=0.004$] (figure 7D). Post-hoc comparisons using the Tukey HSD test indicated that the mean score for the homozygous KO condition) ($M=0.34$, $SEM=0.02$) was significantly different from the wildtype ($M=0.61$, $SEM=0.04$) condition ($p<0.01$). The heterozygous ($M=0.44$, $SEM=0.05$) condition, however, showed no significant differences with either the wildtype or homozygous KO groups. Taken together, these results suggest that the complete removal of lynx1 is detrimental to axon fiber retention during aging. Partial loss of lynx1, however, is apparently sufficient to support neuronal health, even after prolonged periods of reduction (figure 7D).

In order to compare the loss of neuronal cell bodies within the striatum in the 13 month old wildtype, heterozygous lynx1KO, and lynx1KO mice, we performed immunocytochemical analysis of the dorsal striatum using anti-NeuN to label neuronal cell bodies (figure 8). We quantified the NeuN positive cells in wildtype (figure 8A) vs. heterozygous lynx1KO (figure 8B) and lynx1KO (figure 8C) brain sections of the striatal neuropil. There was a significant effect of genotype on neuronal cell body number at 13 months, at the $p<0.05$ level for the three conditions [$F(2,21)= 19.8$, $p<0.0001$] (figure 8D). Post-hoc comparisons using the Tukey HSD test indicated that the mean score for the homozygous KO condition ($M=960$,

SD 85.8) was significantly different from the wildtype (M=1194, SD 93.9) and the heterozygous (M=1171, SD 63.2) conditions. There were no significant differences, however, between the wildtype vs. heterozygous groups. Taken together, these results suggest the complete removal of the lynx1 is detrimental to striatal neuronal health. This observation could explain why, in the dorsal striatum of wildtype mice and heterozygous mice, axon bundles run in compact fascicles, which show distinct boundaries, but in aged lynx1KO mice the boundaries of fascicles become indistinct.

Striatal degeneration as a trigger for vacuole formation

The external degeneration observed in 13 month old animals might have triggered the loss of axon bundles, producing the vacuoles observed in the previous study (Miwa et al., 2006). We suggest here that fascicles may have been lost when the samples in the previous study were switched suddenly from high to low osmolarity in the solution. This change in osmolarity could be associated with a transient phase of ‘curling’ in the previous study during the staining procedure. In summary, we observed two major differences in the aged lynx1KO brain. One is the degeneration of the striatal neuropil, while the other is the degeneration within axons of fascicular fibers coursing through the striatum. The most extreme ultrastructural change manifested itself at 13 months of age, while 1 and 3 month old lynx1KO mice exhibited little to no difference in neuronal structures. The similarity between wildtype and heterozygous samples suggests that lynx1 is protective to neurons, even at half dosage of the protein.

Discussion

We characterized the dorsal striatum morphologically and found changes in the cellular ultrastructure of the lynx1KO mouse brain compared to wildtype mouse brains during aging. Before one year of age we saw no substantial difference between wildtype and lynx1KO mouse brains. In 13 month old lynx1KO animals, however, there was evidence of altered morphology of the fascicles and their integrity appeared weakened. In montages of the fascicles, the density of fiber packing was reduced in lynx1KO mice, and there was evidence of clearing of both nerve fibers and neuronal cell bodies. In this study, we therefore asked what would be the consequence of restricting the degree of lynx1 inhibition over the cholinergic system, and capitalized on the partial lynx1 dosage within heterozygous lynx1KO mice to carry out our investigations. We found that with partial lynx1 reduction it is possible to ameliorate the neuronal loss associated with the aging lynx1KO brains.

Types of altered morphology between and within axons

The external degeneration observed in 13 month old animals might have triggered the loss of axon bundles, producing the vacuoles observed in the previous study. The fact that this was observed only in the lynx1KO mice suggests that the tissue was weakened or cleared out by the degeneration. To summarize the idea that the observed morphology of lynx1KO degeneration within the striatum could lead to weakened fascicle structure, we represented each individual axon by a cotton-tipped swab, and each fascicle by bundles of swabs (figure 9A & B). The wildtype and heterozygous axons are regular and parallel, represented by parallel swabs (figure 9A). In contrast, the lynx1KO axons are skewed (figure 9B), perhaps

because the loss of neuronal cell bodies and clearing of dendritic tissues decreases the external mechanical constraints that force the packing of the fascicles. Furthermore, we saw the altered ultrastructure of axoplasm in the dorsal striatum. This alteration may signify that pathology is transported via axoplasmic flow from defects or signals that originate in cell bodies located outside the striatum.

Age-related changes in cholinergic signaling

Aging is associated with changes in cholinergic signaling (Terry and Buccafusco, 2003) (Albuquerque et al., 2009) and loss of cholinergic neurons (Decker and McGaugh, 1991; Schliebs and Arendt, 2011), as well as loss of axons of cholinergic neurons (Geula et al., 2008). The aging brain may also be harmed by heightened nicotinic acetylcholine receptor function, which could generate excessive calcium signaling. As nicotinic receptor modulators, lynx1 molecules may be required to balance nicotinic receptor activity in the aging brain. We have reported elevated baseline Ca^{2+} levels and elevated nicotine-evoked Ca^{2+} transients in primary neuronal cultured neurons from lynx1KO mice (Miwa et al., 2006). This is consistent with the demonstrated ability of nicotinic receptors to flux Ca^{2+} directly (Colquhoun and Patrick, 1997; Yamauchi et al., 2011), or to induce the release of Ca^{2+} from intracellular calcium stores via downstream effectors (Stevens et al., 2003; Vijayaraghavan et al., 1992). In addition to displaying elevations in Ca^{2+} levels, lynx1KO neurons are more susceptible to toxic levels of glutamate. Pre-incubating neurons with low doses of nicotine fails to protect lynx1KO mouse neurons, whereas this neuroprotective process is robust in wildtype neurons (Miwa et al., 2006). This suggests that lynx1 is playing a critical role in protecting neurons via nicotinic receptor mediated Ca^{2+} dynamics. Elevated intracellular Ca^{2+} levels and exaggerated responses of nicotinic acetylcholine receptors in the lynx1KO mouse would make neurons more susceptible to insults over time. A definitive mechanism of action for the degenerative pathway awaits further investigation.

Genetic, biochemical, and pharmacological studies have demonstrated that nicotinic receptors are downstream effectors of lynx1. The striatal degeneration observed at the light microscopic level was ameliorated by crossing the lynx1KO mice to the $\alpha 7$ and $\beta 2$ KO mouse lines (Miwa et al., 2006). This indicates that lynx operates through both subtypes, in line with evidence that lynx1 can form stable interactions with both subtypes in binding studies (Ibanez-Tallon et al., 2002). As further support for pan-specific interactions with nicotinic receptors, pharmacological agents blocking both subtypes, when given as a cocktail, can block plasticity effects in lynx1KO mice (Morishita et al., 2010). Multiple nicotinic receptor subtypes in the striatum have been reported in rodents (Hill et al., 1993; Perez et al., 2008; Zhang et al., 1998), primates (McCallum et al., 2006) and humans (Court and Clementi, 1995). $\alpha 7$ (O'Neill et al., 2002; Toulorge et al., 2011), $\beta 2$ (Stevens et al., 2003; Zoli et al., 1999), and other nAChRs (Khwaja et al., 2007) have been implicated in neuroprotection (Quik and Kulak, 2002). The requirements for neuroprotection are influenced by many factors, including developmental stage, receptor subtype, and dosage (Picciotto and Zoli, 2008). Lynx1 appears to be critical for nicotine mediated neuroprotection (Miwa et al., 2006), and thus lynx1 adds another layer of complexity to our understanding of nicotinic receptors and neuroprotection.

The lynx1KO degeneration occurs at therapeutically relevant sites in the brain. The dorsal striatum and the neurons which course through it are important targets for the neuroprotective effects of nicotine. Striatal dopamine has been shown to be sensitive to nicotine neuroprotection (Costa et al., 2001; Dajas et al., 2001). In vitro studies invoke changes in intracellular Ca^{2+} levels (Toulorge et al., 2011). Whereas nerve fibers traversing the striatum were significantly affected, hippocampal sections appeared to be normal at all time-points (data not shown), suggesting this susceptibility was specific to cell type. Even though we have observed marked regional differences in the degeneration in aged lynx1KO mice, these differences do not correlate with areas with the highest levels of lynx1 expression. Lynx1 mRNA levels are highest in select brainstem nuclei, CA3 of the hippocampus, and deep cerebellar nuclear neurons, with moderate levels of expression throughout the entire brain (Miwa et al., 1999). The greatest levels of degeneration seen at the light microscopic level are observed in the dorsal striatum, cerebellar peduncles, brainstem and to a lesser extent, the corpus callosum (Miwa et al., 2006). The selective degeneration in the striatum may reflect a selective vulnerability of these neurons to non cell-autonomous stressors caused by the absence of lynx1.

Evidence is emerging that lynx1 levels can change due to physiologically relevant events and different environmental and network factors (Miwa et al., 2011; Miwa et al., 2012; Pfeffer et al.; Sekhon et al, 2005). The sparing of neurons in heterozygous mice reveals that partial reductions in lynx levels may be well tolerated in the brain. This may provide a demonstration of haplosufficiency of the lynx1 gene with respect to neuronal protection. If this extends to learning and cognitive functions, then the lynx1 gene in the brain may be involved in a trade-off between neuroprotection and augmented learning. If expression levels are altered in specific environmental conditions to optimize this trade-off, the degree of cholinergic tone would be able to change in response to situational or environmental demands.

Acknowledgments

Support Acknowledgements: This work was supported by funds from Tobacco-Related Disease Research Program of the University of California, Grant Number TRDRP19KT-0032 for JMM and RLP, TRDRP22DT-0008 and NIH/NRSA Institutional training grant 5 T32 GM07616 for RLP; US- India BRCP Award - 1R21DA033831 for JMM; R01AG-033954 for HAL and JMM; R41DA032464 and 1R43MH094004 for PK, HB, APW and AW. Financial support for this project included funds for undergraduate research from the College of Arts & Sciences and the Department of Biological Sciences at Lehigh University for KMO. The Jensen electron microscopy facility is funded in part by the Gordon and Betty Moore Foundation, the Agouron Institute and the Beckman Foundation. Special thanks to Dr. Amber Rice for helpful discussion and critical reading of the manuscript, and to Samantha Eichelberger for editorial help. In memory of Andreas Walz.

Bibliography

Albuquerque EX, Pereira EF, Alkondon M, Rogers SW. Mammalian nicotinic acetylcholine receptors: from structure to function. Physiol Rev. 2009; 89:73–120. [PubMed: 19126755]

Berger F, Gage FH, Vijayaraghavan S. Nicotinic receptor-induced apoptotic cell death of hippocampal progenitor cells. J Neurosci. 1998; 18:6871–6881. [PubMed: 9712657]

Bordia T, Campos C, Huang L, Quik M. Continuous and intermittent nicotine treatment reduces L-3,4-dihydroxyphenylalanine (L-DOPA)-induced dyskinesias in a rat model of Parkinson's disease. J Pharmacol Exp Ther. 2008; 327:239–247. [PubMed: 18650244]

Colquhoun LM, Patrick JW. Pharmacology of neuronal nicotinic acetylcholine receptor subtypes. Adv Pharmacol. 1997; 39:191–220. [PubMed: 9160116]

Costa G, Abin-Carriquiry JA, Dajas F. Nicotine prevents striatal dopamine loss produced by 6-hydroxydopamine lesion in the substantia nigra. Brain Res. 2001; 888:336–342. [PubMed: 11150495]

Court J, Clementi F. Distribution of nicotinic subtypes in human brain. Alzheimer Dis Assoc Disord. 1995; 9(Suppl 2):6–14. [PubMed: 8534425]

Cragg B. Preservation of extracellular space during fixation of the brain for electron microscopy. Tissue Cell. 1980; 12:63–72. [PubMed: 6987773]

Dajas-Bailador FA, Lima PA, Wonnacott S. The alpha7 nicotinic acetylcholine receptor subtype mediates nicotine protection against NMDA excitotoxicity in primary hippocampal cultures through a Ca(2+) dependent mechanism. Neuropharmacology. 2000; 39:2799–2807. [PubMed: 11044750]

Dajas F, Costa G, Abin-Carriquiry JA, McGregor R, Urbanavicius J. Involvement of nicotinic acetylcholine receptors in the protection of dopamine terminals in experimental parkinsonism. Funct Neurol. 2001; 16:113–123. [PubMed: 11996506]

Decker MW, McGaugh JL. The role of interactions between the cholinergic system and other neuromodulatory systems in learning and memory. Synapse. 1991; 7:151–168. [PubMed: 1672782]

Geula C, Nagykery N, Nicholas A, Wu CK. Cholinergic neuronal and axonal abnormalities are present early in aging and in Alzheimer disease. J Neuropathol Exp Neurol. 2008; 67:309–318. [PubMed: 18379437]

Huang LZ, Abbott LC, Winzer-Serhan UH. Effects of chronic neonatal nicotine exposure on nicotinic acetylcholine receptor binding, cell death and morphology in hippocampus and cerebellum. Neuroscience. 2007; 146:1854–1868. [PubMed: 17434679]

Ibanez-Tallon I, Miwa JM, Wang HL, Adams NC, Crabtree GW, Sine SM, Heintz N. Novel modulation of neuronal nicotinic acetylcholine receptors by association with the endogenous prototoxin lynx1. Neuron. 2002; 33:893–903. [PubMed: 11906696]

Kaneko S, Maeda T, Kume T, Kochiyama H, Akaike A, Shimohama S, Kimura J. Nicotine protects cultured cortical neurons against glutamate-induced cytotoxicity via alpha7-neuronal receptors and neuronal CNS receptors. Brain Res. 1997; 765:135–140. [PubMed: 9310404]

Khwaja M, McCormack A, McIntosh JM, Di Monte DA, Quik M. Nicotine partially protects against paraquat-induced nigrostriatal damage in mice; link to α6β2* nAChRs. J Neurochem. 2007; 100:180–190. [PubMed: 17227438]

Levin ED, McClernon FJ, Rezvani AH. Nicotinic effects on cognitive function: behavioral characterization, pharmacological specification, and anatomic localization. Psychopharmacology (Berl). 2005:1–17.

McCallum SE, Parameswaran N, Bordia T, Fan H, Tyndale RF, Langston JW, McIntosh JM, Quik M. Increases in α4* but not α3*/α6* nicotinic receptor sites and function in the primate striatum following chronic oral nicotine treatment. J Neurochem. 2006; 96:1028–1041. [PubMed: 16412091]

Miwa JM, Freedman R, Lester HA. Neural systems governed by nicotinic acetylcholine receptors: emerging hypotheses. Neuron. 2011; 70:20–33. [PubMed: 21482353]

Miwa JM, Ibanez-Tallon I, Crabtree GW, Sanchez R, Sali A, Role LW, Heintz N. lynx1, an endogenous toxin-like modulator of nicotinic acetylcholine receptors in the mammalian CNS. Neuron. 1999; 23:105–114. [PubMed: 10402197]

Miwa JM, Stevens TR, King SL, Caldarone BJ, Ibanez-Tallon I, Xiao C, Fitzsimonds RM, Pavlides C, Lester HA, Picciotto MR, et al. The Prototoxin lynx1 Acts on Nicotinic Acetylcholine Receptors to Balance Neuronal Activity and Survival In Vivo. Neuron. 2006; 51:587–600. [PubMed: 16950157]

Morishita H, Miwa JM, Heintz N, Hensch TK. Lynx1, a cholinergic brake, limits plasticity in adult visual cortex. Science. 2010; 330:1238–1240. [PubMed: 21071629]

O'Neill MJ, Murray TK, Lakics V, Visanji NP, Duty S. The role of neuronal nicotinic acetylcholine receptors in acute and chronic neurodegeneration. Curr Drug Targets CNS Neurol Disord. 2002; 1:399–411. [PubMed: 12769612]

Orb S, Wieacker J, Labarca C, Fonck C, Lester HA, Schwarz J. Knockin mice with Leu9'Ser α4 nicotinic receptors: substantia nigra dopaminergic neurons are hypersensitive to agonist and lost postnatally. Physiol Genomics. 2004; 18:299–307. [PubMed: 15199190]

Orr-Urtreger A, Broide RS, Kasten MR, Dang H, Dani JA, Beaudet AL, Patrick JW. Mice homozygous for the L250T mutation in the 7 nicotinic acetylcholine receptor show increased neuronal apoptosis and die within 1 day of birth. J Neurochem. 2000; 74:2154–2166. [PubMed: 10800961]

Picciotto MR. Nicotine as a modulator of behavior: beyond the inverted U. Trends Pharmacol Sci. 2003; 24:493–499. [PubMed: 12967775]

Picciotto MR, Zoli M. Neuroprotection via nAChRs: the role of nAChRs in neurodegenerative disorders such as Alzheimer's and Parkinson's disease. Front Biosci. 2008; 13:492–504. [PubMed: 17981563]

Picciotto MR, Zoli M, Lena C, Bessis A, Lallemand Y, LeNovere N, Vincent P, Pich EM, Brulet P, Changeux JP. Abnormal avoidance learning in mice lacking functional high-affinity nicotine receptor in the brain. Nature. 1995; 374:65–67. [PubMed: 7870173]

Quik M, Cox H, Parameswaran N, O'Leary K, Langston JW, Di Monte D. Nicotine reduces levodopa-induced dyskinesias in lesioned monkeys. Ann Neurol. 2007; 62:588–596. [PubMed: 17960553]

Quik M, Kulak JM. Nicotine and nicotinic receptors; relevance to Parkinson's disease. Neurotoxicology. 2002; 23:581–594. [PubMed: 12428730]

Ryan RE, Ross SA, Drago J, Loiacono RE. Dose-related neuroprotective effects of chronic nicotine in 6-hydroxydopamine treated rats, and loss of neuroprotection in α4 nicotinic receptor subunit knockout mice. Br J Pharmacol. 2001; 132:1650–1656. [PubMed: 11309235]

Schliebs R, Arendt T. The cholinergic system in aging and neuronal degeneration. Behav Brain Res. 2011; 221:555–563. [PubMed: 21145918]

Stevens TR, Krueger SR, Fitzsimonds RM, Picciotto MR. Neuroprotection by nicotine in mouse primary cortical cultures involves activation of calcineurin and L-type calcium channel inactivation. J Neurosci. 2003; 23:10093–10099. [PubMed: 14602824]

Tekinay AB, Nong Y, Miwa JM, Lieberam I, Ibanez-Tallon I, Greengard P, Heintz N. A role for LYNX2 in anxiety-related behavior. Proc Natl Acad Sci U S A. 2009; 106:4477–4482. [PubMed: 19246390]

Terry AV Jr, Buccafusco JJ. The cholinergic hypothesis of age and Alzheimer's diseaserelated cognitive deficits: recent challenges and their implications for novel drug development. J Pharmacol Exp Ther. 2003; 306:821–827. [PubMed: 12805474]

Toulorge D, Guerreiro S, Hild A, Maskos U, Hirsch EC, Michel PP. Neuroprotection of midbrain dopamine neurons by nicotine is gated by cytoplasmic Ca2+ FASEB J. 2011; 25:2563–2573. [PubMed: 21507900]

Vijayaraghavan S, Pugh PC, Zhang ZW, Rathouz MM, Berg DK. Nicotinic receptors that bind α-bungarotoxin on neurons raise intracellular free Ca^{2+} Neuron. 1992; 8:353–362. [PubMed: 1310863]

Yamauchi JG, Nemecz A, Nguyen QT, Muller A, Schroeder LF, Talley TT, Lindstrom J, Kleinfeld D, Taylor P. Characterizing ligand-gated ion channel receptors with genetically encoded Ca2++ sensors. PLoS One. 2011; 6:e16519. [PubMed: 21305050]

Zoli M, Picciotto MR, Ferrari R, Cocchi D, Changeux JP. Increased neurodegeneration during ageing in mice lacking high-affinity nicotine receptors. Embo J. 1999; 18:1235–1244. [PubMed: 10064590]

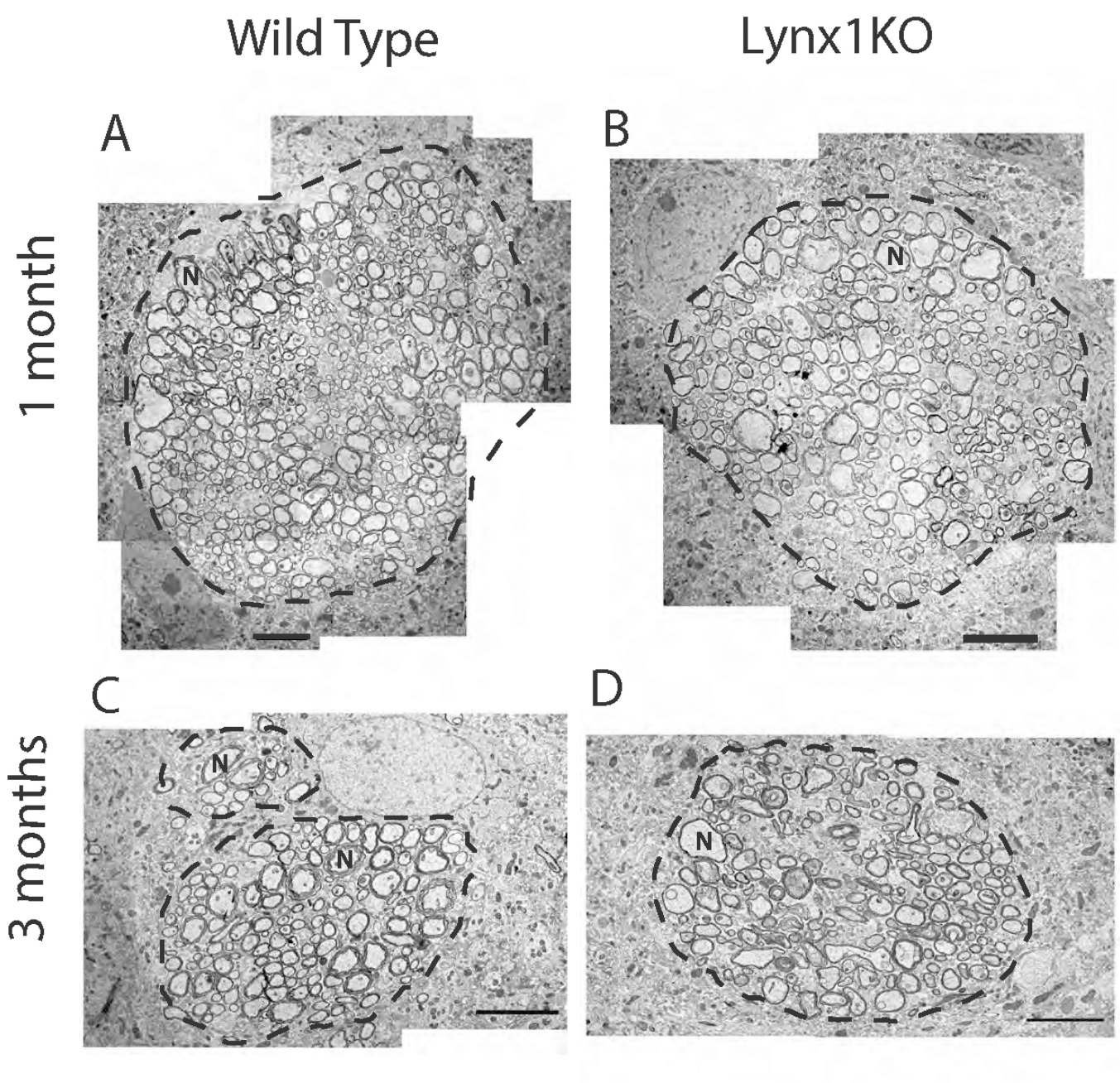

Figure 1.

Electron micrographs of fascicles in the dorsal striatum of 1 month old and 3 month old-mice in cross section. In young striatal bundles, the nerve fibers (marked as N) are closely packed for both wildtype and lynx1KO mouse, so that the boundary of an individual bundle is clearly demarcated (indicated with a dashed line). These schematic images are shown in Figure 9A. (1A) Ultrastructural montage of a nerve fiber bundle of a 1 month old wildtype mouse. (1B) Ultrastructural montage of a nerve fiber bundle of a 1 month old lynx1KO mouse. (1C) Ultrastructural montage of a nerve fiber bundle of a 3 month old wildtype

mouse. (1D) Ultrastructural montage of a nerve fiber bundle of a 3 month old lynx1KO. All scale bars = 5 μm.

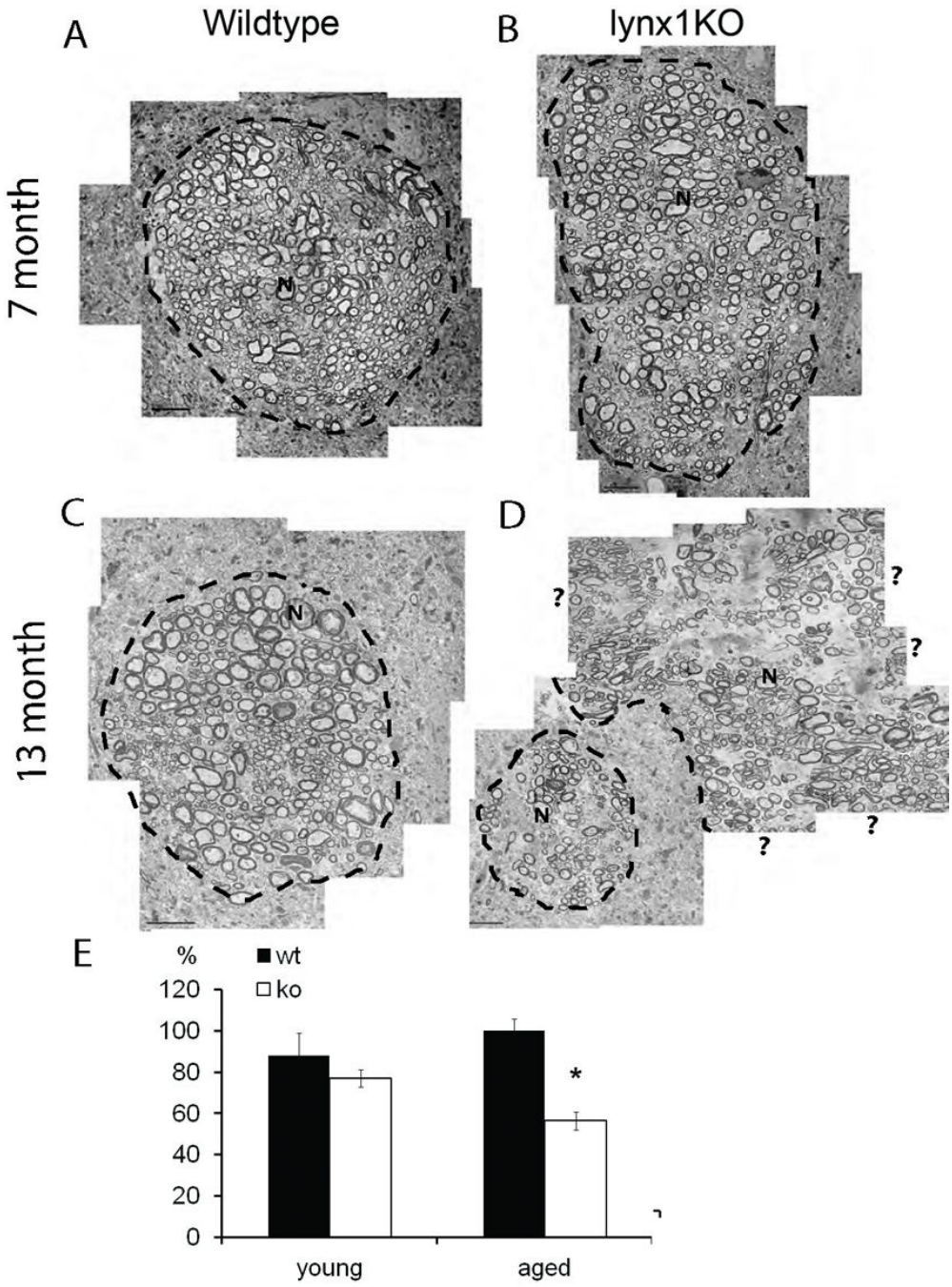

Figure 2.

Electron micrograph of a nerve fiber bundle in dorsal striatum of 7- and 13-month-oldmice in cross section, for both wildtype and lynx1KO. In 13-month-old striatal bundles from wild-type animals, the nerve fibers (N) are still tightly packed, as drawn with *dashed lines*. However, the nerve fibers from the 7-month-old lynx1KO mice appear slightly dispersed and the 13-month-old lynx1KO fibers appear to be highly dispersed. **a** Ultrastructural montage of a nerve fiber bundle of a 7-month-old wild type. **b** Ultrastructural montage of a nerve fiber bundle from a 7-month-old lynx1KO mouse. **c** Ultrastructural montage of a

nerve fiber bundle from a 13-month-old wild type animal. **d** Ultrastructural montage of a nerve fiber bundle from a 13-month-old lynx1KO. Although some of the bundles (*lower left fascicle*) appear to be packed, many (*upper right*) have lost their shape so that the boundary cannot be easily demarcated (shown by the "?" marks). *All scale bars* 5 μm. **e** Bar graph of nerve fiber density in a fascicle (# of nerve fibers per μm^2). [$F(3,11)=6.11$, $p<0.01$] by ANOVA. Post-hoc Tukey test indicates a significant difference in the mean when comparing the 13-month-old lynx1KO fiberdensity (56.4±9.3%, n=3) to that in 13-month-old wild-type (100.0 ± 5.8%, n=5). Densities in young wild-type (88.2 ±11.0%, n=4) and young lynx1KO samples (77.1 ± 4.2%, n=3) were not significantly different. y-axis is in %, data normalized to the 13-month-old wild-type nerve fiber density.

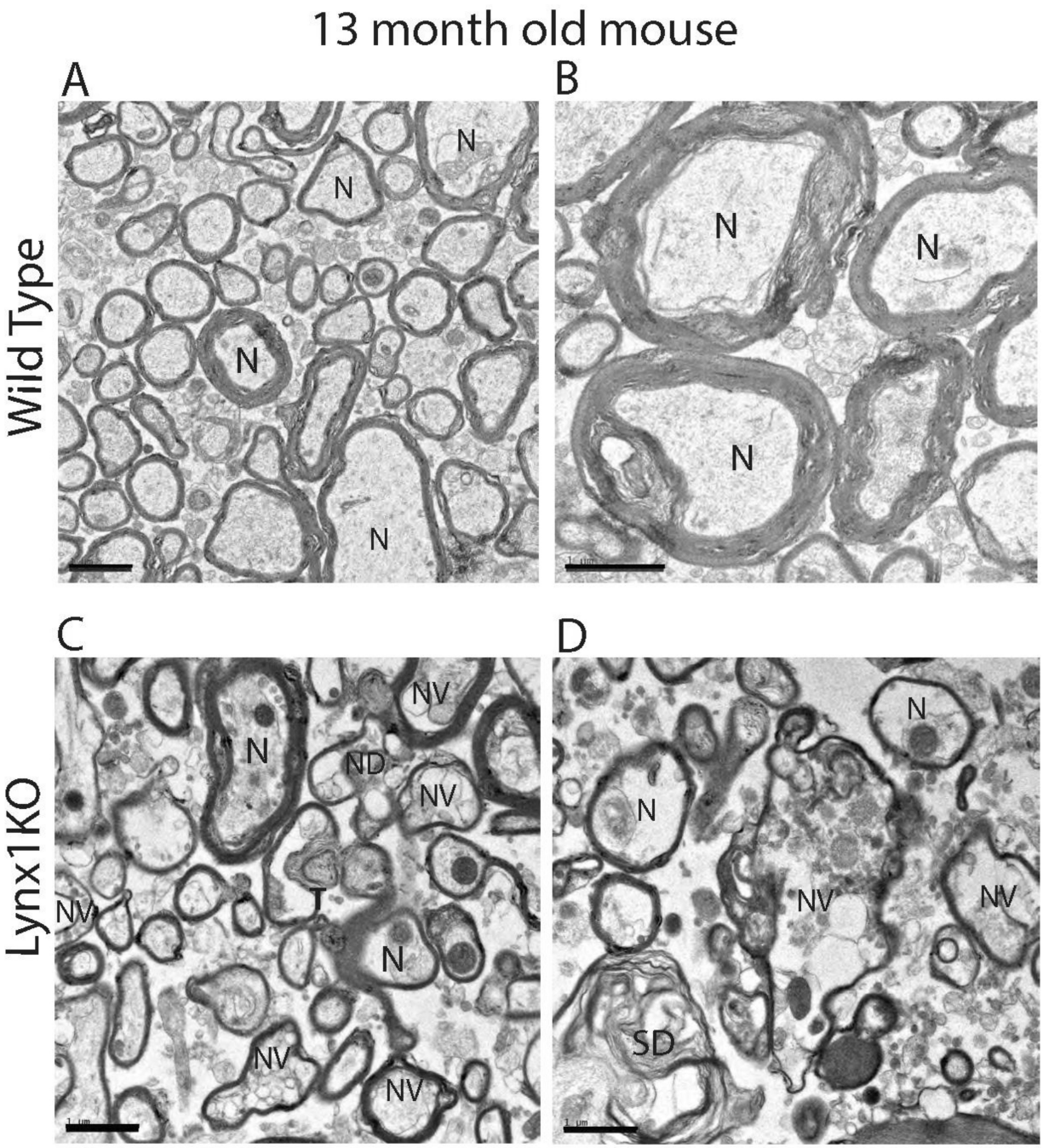

Figure 3.

Nerve fibers in the fascicles are markedly disrupted in lynx1KO mice. High power micrographs of the 13 month old lynx1KO striatal fascicles reveals marked disruption in the region between individual nerve fibers. In some cases, the diameters of the axons themselves, or the myelin sheaths surrounding them, appeared shrunken. In some cases the myelin appear to be degenerated (marked as SD), and the interior of the axon appears vacuolated (marked as NV). (3A) 13 month old wildtype mouse brain. (3B) 13 month old

wildtype mouse brain, higher power. (3C) 13 month old lynx1KO mouse brain. (3D) 13 month old lynx1KO mouse brain, higher power. *All scale bars are 1um*.

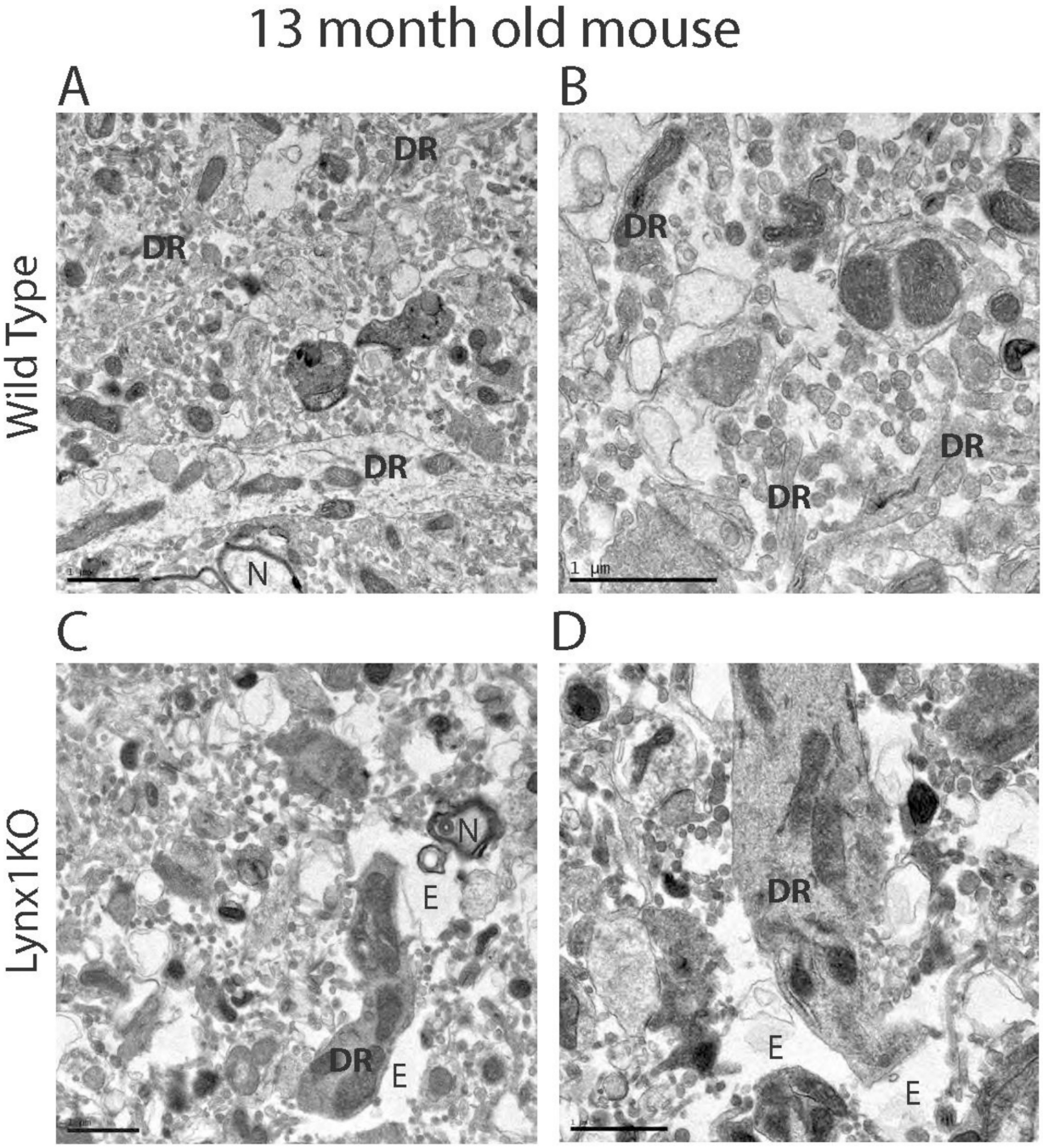

Figure 4.

Microscopic examination of 13 month old striatal neuropil. (4A) Electron micrograph of wildtype mouse. Part of an individual nerve fiber (marked as N) is shown at bottom. (4B) Electron micrograph of wildtype mouse at higher magnification. For wildtype animals, the nerve fiber bundles are still packed by parts of dendritic (marked as DR) and neuronal cell bodies. (4C) Electron micrograph of lynx1KO mouse. (4D) Electron micrograph of lynx1KO mouse at higher magnification. The tissues in the lynx1KO mouse contain many

areas that lack intracellular structures as compared to the wildtype mice. Areas between the dendrites appear empty (marked as E). All scale bars = 1μm.

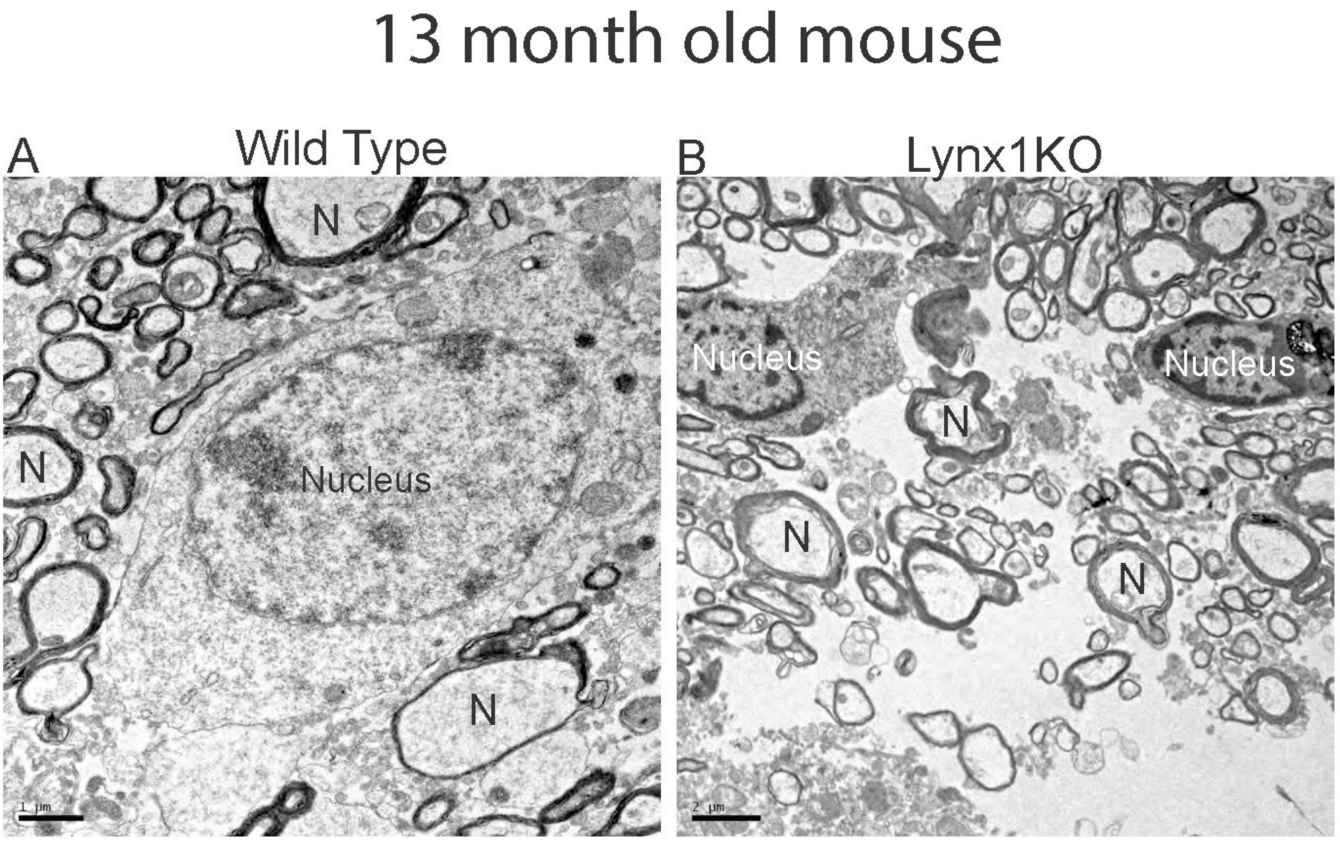

Figure 5.

Electron micrograph of the somatic structures in the striatal neuropil between fascicles show disruption of nuclei evident in aging lynx1KO brains. Lynx1KO samples appear to contain condensed and clear nuclei, and empty spaces between nerve structures in the striatum. (5A) 13 month old wildtype striatum. (5B) 13 month old lynx1KO striatum. Cell nuclei appear condensed or cleared. *All scale bars are 1um*.

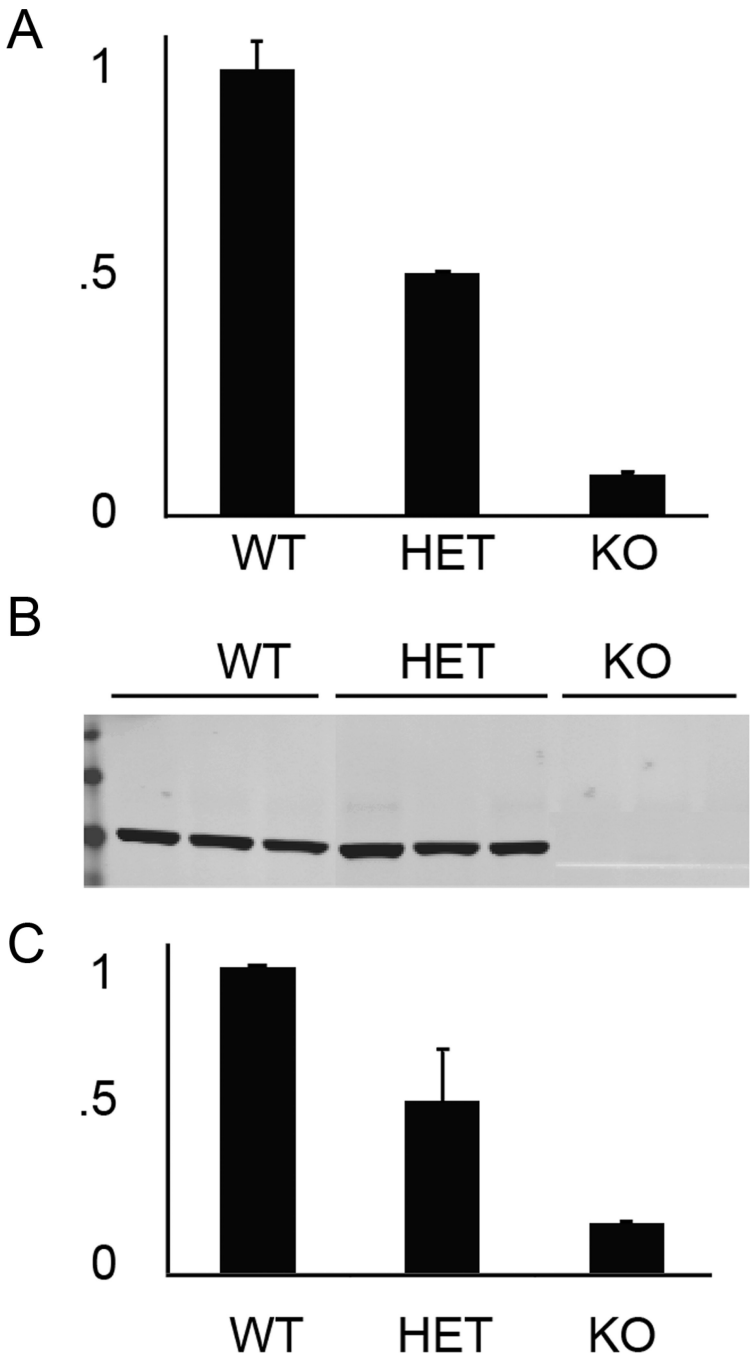

Figure 6.

Measurements of lynx1 levels using qPCR and Western analyses. (6A) qPCR analysis indicates 50% of the transcript levels in heterozygous lynx1KO mice as compared to those of wildtype mice. y-axis is fold level of expression of lynx1 relative to wildtype levels. (6B) Western blot of total brain protein extracts from 13 month old mice, run out in triplicate and detected with anti-lynx1 antibodies. (6C) Quantitation of lynx1 bands indicates protein levels in the heterozygous mice that are ~50% of wildtype levels, and is absent in

homozygous lynx1KO extracts. y-axis is fold level of lynx protein relative to wildtype levels.

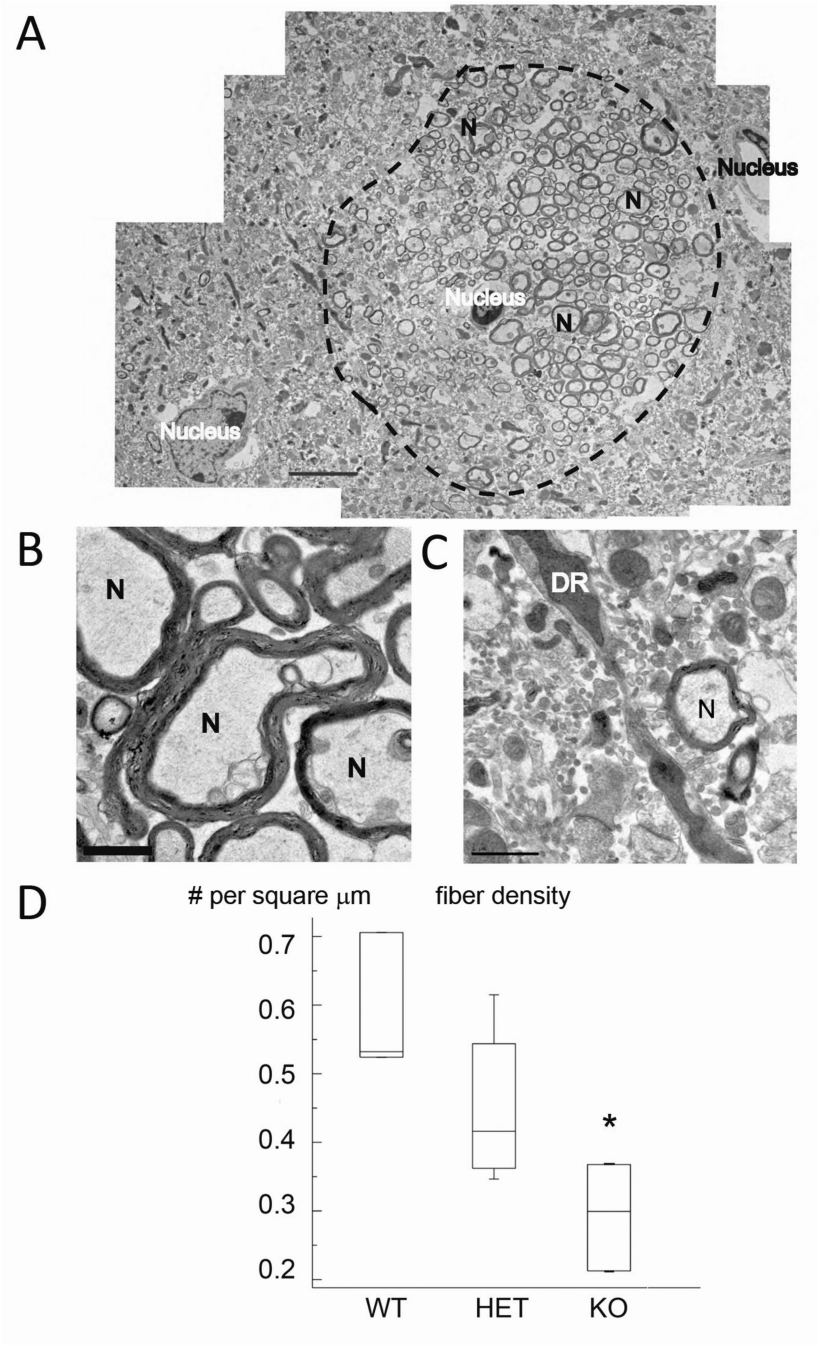

Figure 7.

Microscopic examination of 13 month old heterozygous lynx1KO mice reveals that titrating lynx1 dosage protects neurons. (7A) The nerve fibers (marked as N) are closely packed in heterozygous lynx1KO mice, so that the boundary of an individual bundle is clearly demarcated (indicated with a dashed line). These schematic images are shown in Figure 9A. (7B) Part of an individual nerve fiber (marked as N) is shown. (7C) Electron micrograph of the somatic structures in the striatal neuropil between fascicles shows that the nerve fibers (marked as N) are still packed by the parts of dendritic structures (marked as DR). (7D) Bar

graph of axon fiber density. y-axis is number of axons in a fascicle/area in μm^2. Wildtype is 0.61 ± 0.04, n=4, heterozygous lynx1KO 13 month old is 0.44 ± 0.05, n=5, and lynx1KO is 0.34 ± 0.02, n=3. $F(2,9)= 6.57$, $p < 0.01$)].

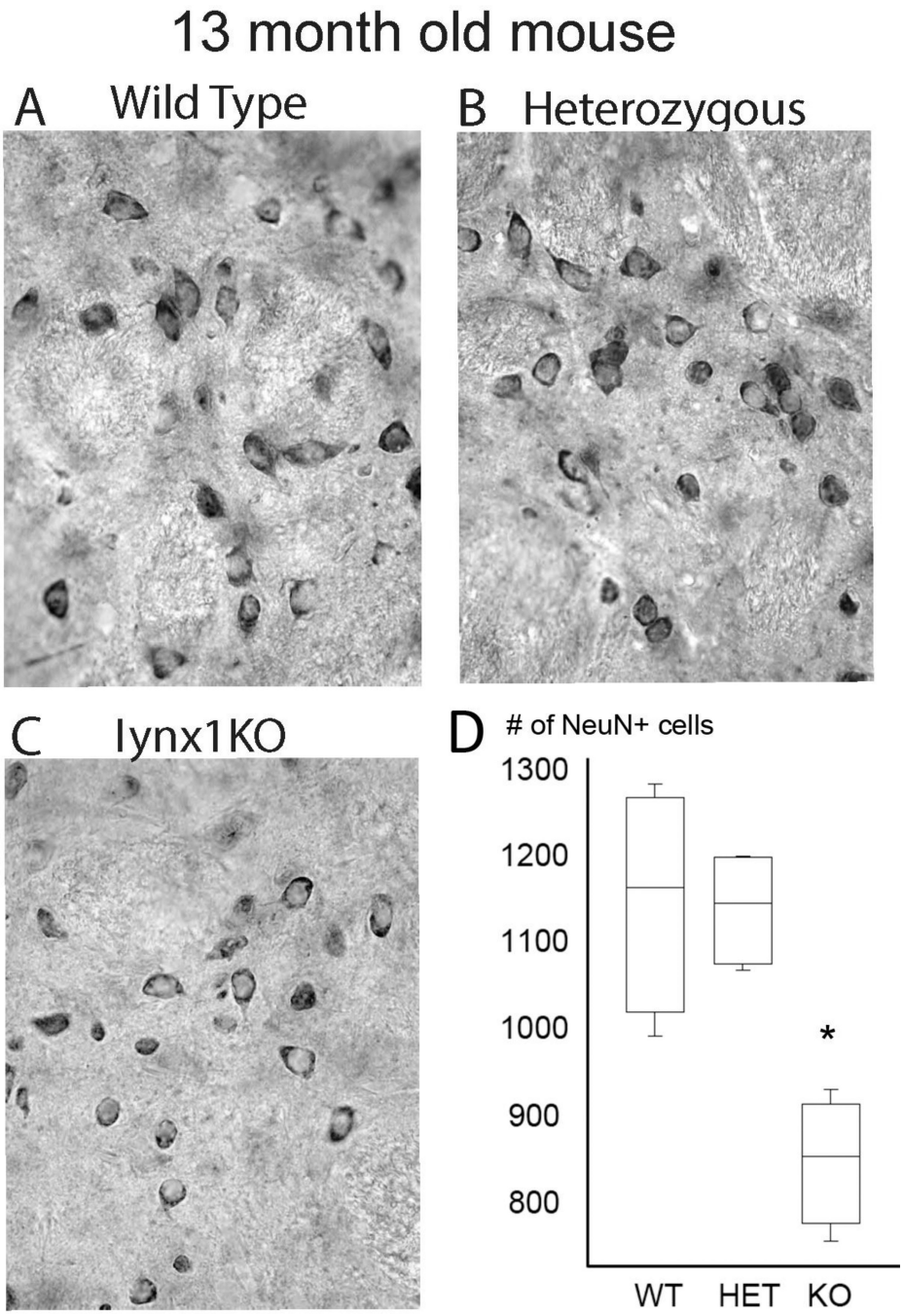

Figure 8.

Neurons are lost in aging dorsal striatum of lynx1KO mice, but titrating lynx dosage protects neurons. All images taken at 63x magnification. (8A) 13 month old wildtype mouse brain stained with neuronal marker NeuN. (8B) 13 month old heterozygous lynx1KO mouse brain stained with NeuN. (8C) 13 month old lynx1KO mouse brain stained with NeuN. (8D) Box plot of number of neurons as assessed by NeuN positive staining. y-axis plots number of NeuN positive neurons per region.

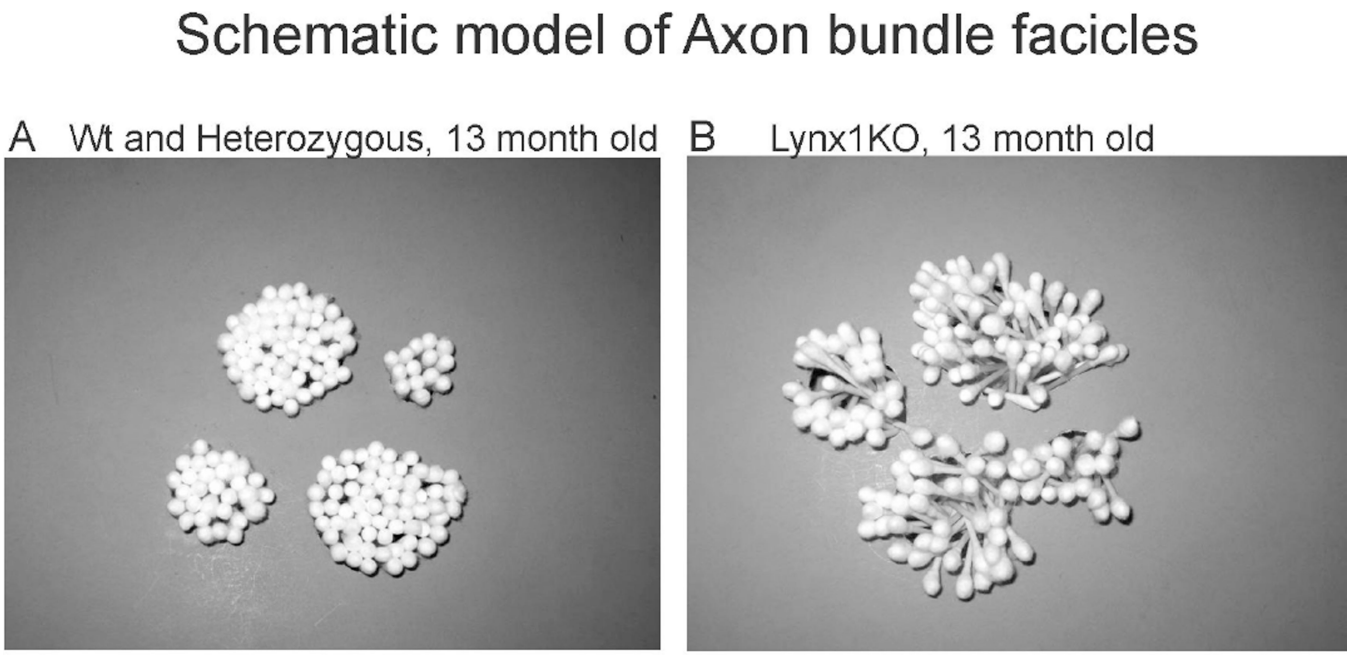

Figure 9.

Schematic models of axon bundle fascicles of (9A) 13 month old wildtype and heterozygous lynx1KO mice, and (9B) the dispersed bundles of 13 month old homozygous lynx1KO, illustrated by the clumping of cotton-tipped swabs which represent myelinated axon fibers.